Journal of Biological Systems, Vol. 25, No. 4 (2017) 625–655

DOI: 10.1142/S0218339017400058

World Scientific
www.worldscientific.com

PREVENTING THE SPREAD OF SCHISTOSOMIASIS IN GHANA: POSSIBLE OUTCOMES OF INTEGRATED OPTIMAL CONTROL STRATEGIES

HONG ZHANG

Department of Financial Mathematics
Jiangsu University, ZhenJiang, JiangSu 212013, P. R. China
hongzhang@ujs.edu.cn

PRINCE HARVIM

Faculty of Science, Jiangsu University
ZhenJiang, JiangSu 212013, P. R. China
princeharvim@yahoo.com

PAUL GEORGESCU*

Department of Mathematics
Technical University of Iaşi, Bd. Copou 11A
700506 Iaşi, Romania
v.p.georgescu@gmail.com

Received 26 January 2017
Accepted 3 August 2017
Published 29 November 2017

The goal of a future free from schistosomiasis in Ghana can be achieved through integrated strategies, targeting simultaneously several stages of the life cycle of the schistosome parasite. In this paper, the transmission of schistosomiasis is modeled as a multi-scale 12-dimensional system of ODEs that includes vector-host and within-host dynamics of infection. An explicit expression for the basic reproduction number R_0 is obtained via the next generation method, this expression being interpreted in biological terms, as well as in terms of reproductive numbers for each type of interaction involved. After discussing the stability of the disease-free equilibrium and the existence and uniqueness of the endemic equilibrium, the Center Manifold Theory is used to show that for values of R_0 larger than 1, but close to 1, the unique endemic equilibrium is locally asymptotically stable. A sensitivity analysis indicates that R_0 is most sensitive to the natural death rate of the vector population, while numerical simulations of optimal control strategies reveal that the most effective strategy for the control and possible elimination of schistosomiasis should combine sanitary measures (access to safe water, improved sanitation and hygiene education), large-scale treatment of infected population and vector control measures (via the use of molluscicides), for a significant amount of time.

Keywords: Schistosomiasis; Stability Analysis; Basic Reproduction Number; Sensitivity Index; Optimal Control.

*Corresponding author.

1. Introduction

Schistosomiasis (also known as bilharziasis and snail fever) is a parasitic disease caused by trematode worms of the genus *Schistosoma*.[1] There are many species of *Schistosoma*, but only five of them are known to infect humans and more than 90% of all infections are caused by just three of those five, namely, *Schistosoma mansoni* (mainly in Africa and South America) and *Schistosoma japonicum* (mainly in China and the Philippines), which produce intestinal schistosomiasis, and *Schistosoma haematobium* (common in Africa and some countries in the Middle East), which produces urinary schistosomiasis.[2] The other two less common species adapted to humans are *Schistosoma intercalatum* (in Africa) and *Schistosoma mekongi* (in Cambodia and Laos).[3]

Schistosomiasis is the second most devastating of all parasitic human diseases, surpassed only by malaria,[4] having caused an estimated loss of 24–29 million disability-adjusted life years (DALYs) in 2010.[5] Also, 240,000 deaths are annually attributed to schistosomiasis.[6] In 2014, an estimated total of 255 million people residing in 78 countries were at a high risk of infection, no vaccines being available for the disease.[7]

Schistosomiasis is transmitted to humans when free swimming parasitic larvae (cercariae) penetrate the skin of people exposed to infected freshwater. Skin penetration by cercariae is often followed by itchiness, with a rash at the site of cercarial penetration on the skin.[8] Katayama fever, which is an early clinical manifestation of schistosomiasis, occurs as a results of migration of schistosomula through the blood or the lymphatic system,[9] within 2–12 weeks after the primary exposure to contaminated water.[10] Katayama fever has flu-like symptoms such as fever, fatigue, myalgia, headache and cough.[11]

Bladder cancer, liver fibrosis, ascites and hypertension are the advanced and late stage consequences of *S. haematobium*.[12] *S. mansoni* and *S. japonicum* cause intestinal schistosomiasis, which leads to bowel obstruction, appendicitis and gastrointestinal perforation.[13] *S. japonicum* is often associated with cerebral granulomatous lesions leading to epilepsy, paralysis and meningoencephalitis.[14] Also, schistosomiasis infections cause growth retardation, anaemia, cognitive impairment and memory deficit in children.[15] All *Schistosoma* species demonstrate narrow specificity for their intermediate hosts. In this regard, *S. mansoni* infects *Biomphalaria* (large flat spiral snails), *S. japonicum* and *S. mekongi* infect *Oncomelania* (small elongate snails), while *S. haematobium* and *S. intercalatum* infect *Bulinus* (medium ovoid snails). Further details regarding the transmission cycle of schistosomiasis and its possible consequences are discussed, for instance, in Refs. 16, 17, 18 and 20.

The current schistosomiasis control strategies include large-scale drug treatment of infected populations with praziquantel (PZQ), promoting health education, improving access to safe water and sanitation, together with vector control

measures, by reducing the vector (snail) population through the use of molluscicides. However, large-scale drug administration, which is currently the main control strategy, does not prevent reinfection, and infection rates tend to return to high values within 24 months.[21] Also, the onset of resistance of some snail species to molluscicides calls for a better understanding of the process of disease transmission and a development of integrated control strategies for the prevention and control of schistosomiasis.

The disease is endemic in Ghana, being widespread across all 10 regions of this country.[2] From Figs. 1 and 2, one may observe that *S. haematobium* is highly endemic in all parts of the country while *S. mansoni* is highly endemic in the western and upper east regions. Several attempts to estimate the population infected or at risk of contracting schistosomiasis in Ghana have been made in the last decade. In 2008, it was estimated that 8.5 million were at high risk of infection with schistosomiasis out of a total population of about 23.8 million, while in 2010, this number increased to 9.5 million.[22]

The mathematical modeling of infectious diseases has become an important tool in understanding the dynamics of disease transmission and in decision making regarding intervention programs for disease control. The first mathematical models of schistosomiasis were developed in 1965.[24,25] Those models influenced subsequent modeling approaches (see Refs. 26–29).

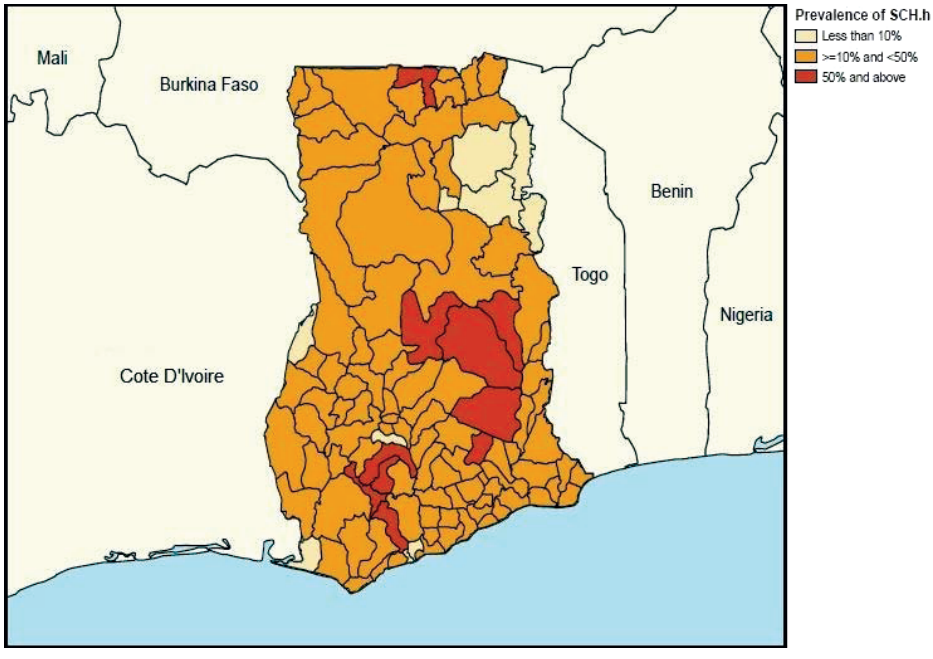

Fig. 1. Endemic areas of *S. haematobium* in Ghana as of 2015 (data obtained from Ref. 23).

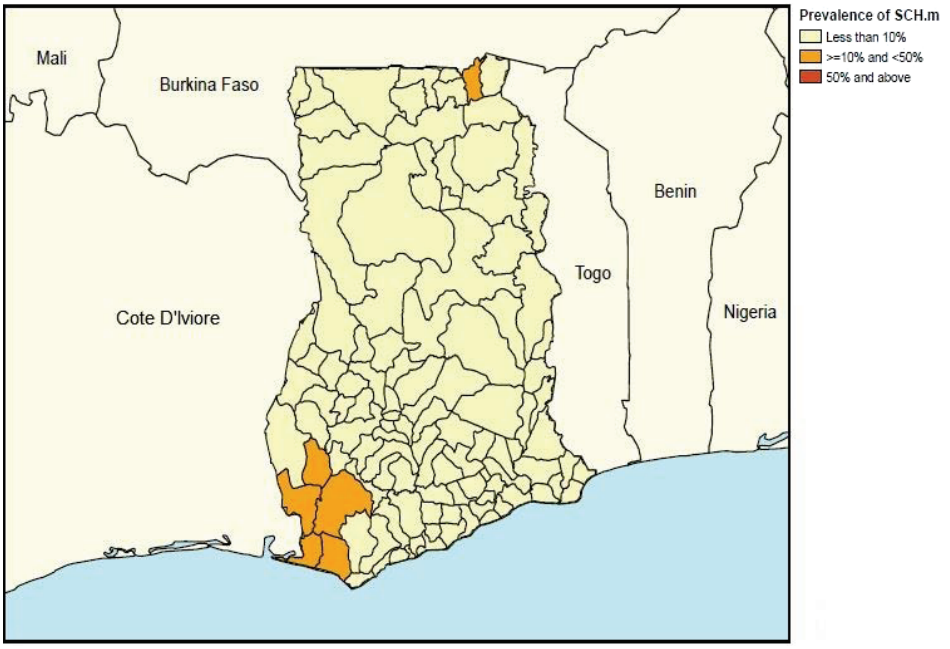

Fig. 2. Endemic areas of *S. mansoni* in Ghana as of 2015 (data obtained from Refs. 23).

Many of the earlier models focused only on the transmission of the disease in human and vector populations. However, a model in which time delay is used to describe the dynamics of schistosomes has recently been proposed in Ref. 30. This model keeps track of multiple resistant schistosome strains, of the mating structure of the parasite and of the biological complexity associated with the life cycle of the parasite. A global analysis of a model of schistosomiasis transmission which is subject to biological control has been carried out in Ref. 31. Mathematical models tracing the life of cercariae from the moment they enter the body up to the egg production stage and the type of immune responses to infection have been constructed in Refs. 32 and 33.

The disease has a complex transmission cycle, which makes the parameters associated with disease transmission difficult to estimate. In view of this, research has been conducted on parameter estimation for schistosomiasis transmission. In Ref. 34, the parameters governing the transmission dynamics of schistosomes were given an estimation, while in Ref. 35, the dynamics of infection with *S. japonicum* in villagers of Leyte in the Philippines was modeled and estimated. Temperature and environmental factors have been noted to influence the transmission of schistosomiasis. The impact of long-term temperature changes on the epidemiology and control of schistosomiasis has been investigated in Ref. 36, the disease being noted to be endemic at temperatures between 18°C and 28°C.[39] In Ref. 40, a six-dimensional

model with five time delays was considered, the effect of time delays on transmission dynamics of schistosomiasis being then investigated.

These models have provided useful information for understanding the dynamics of schistosomiasis transmission. However, very few studies on applying optimal control theory to schistosomiasis transmission models have been carried out. Notably, Pontryagin's maximum (minimum) principle[41] can be successfully used for decision making in various applications. In Ref. 42, optimal control methods were used to determine the optimal vaccination strategy to reduce the sizes of the populations of susceptible and infective individuals for a general SIR epidemic model, while in Ref. 43, optimal strategies for a cost-effective control of malaria transmission have been derived. It has been concluded in Ref. 44 that an integrated strategy had the highest impact in the control of *Aedes aegypti* mosquito.

According to Refs. 2 and 16, vaccines for schistosomiasis are still in the fundamental stages of development and mass administration of PZQ, which is the main control measure, cannot prevent reinfection, in addition to causing several other issues. Therefore, an integrated control strategy targeting simultaneously several stages of the life cycle of the schistosome parasite is the sole approach having the potential to eradicate schistosomiasis. It is then meaningful to formulate a mathematical model which is subject to several control strategies in order to determine the impact of integrated control on the dynamics of schistosomiasis transmission in Ghana. To this purpose, we develop a multi-scale mathematical model for schistosomiasis transmission that includes within-host (human) and vector (snail)-host dynamics of infection.

First, we analyze the model without control measures and investigate its stability properties. We perform a sensitivity analysis on the basic reproduction number R_0 to determine the parameters to which R_0 is the most sensitive. Interpreting the results of the sensitivity analysis, we are led to consider three control measures to steer the behavior of the model. Optimal control theory is subsequently used to investigate the effectiveness of integrating the control measures, namely improving access to safe water, sanitation and hygiene education, large-scale treatment of infected population groups and reducing the vector (snail) population by the use of molluscicides, upon the transmission dynamics of schistosomiasis.

The remaining part of the paper is organized as follows. In Sec. 2, we give a description of the within-host and vector-host schistosomiasis transmission models, stating also the biological assumptions and definitions of the various parameters. In Sec. 3, we determine the disease-free and the endemic equilibria, along with an explicit expression of the basic reproduction number. In Sec. 4, we perform a sensitivity analysis on the basic reproduction number. In Sec. 5, we state the control problem as well as the objective functional to be minimized and apply the Pontryagin's minimum principle to find the necessary conditions for the optimal control. In Sec. 6, we complement our theoretical analysis with several numerical simulations. The final conclusions are presented in Sec. 7.

2. Model Formulation

To formulate our model, we employ standard SEI models for both hosts (humans) and vectors (snails), in which we further incorporate the life cycle of the schistosome parasite in two different environments, namely the external environment and the human body (leading to within-host parasite dynamics). The extended model is based on monitoring the dynamics of 12 populations at any time t. These populations are as follows:

- Susceptible humans $S_H(t)$, exposed humans $E_H(t)$ and infected humans $I_H(t)$, for the human hosts;
- Susceptible snails $S_v(t)$, exposed snails $E_v(t)$ and infected snails $I_v(t)$, for the vectors;
- Cercariae $C(t)$ and miracidia $M(t)$, for the parasites in the external environment;
- Cercariae $C_H(t)$, immature schistosome worms $W_I(t)$, mature schistosome worms $W_m(t)$ and worm eggs $e_H(t)$, for the parasites within the humans.

To construct our model, we make the following biological assumptions:

- There is no vertical transmission of schistosomiasis from mother to the newborn child.
- The human population acquire the disease through contact with cercariae $C(t)$ and the vector population acquire the disease through contact with miracidia $M(t)$.
- There is no immigration of infectious humans.
- Infected snails do not reproduce, due to castration by the miracidia, which is due to the consumption of reproductive tissues within the snail hosts to release cercariae.
- There is no immune response in neither snail nor human populations.
- Heterogeneity of host and vector populations, respectively, for disease transmission and progression are not considered.

Humans are recruited into the susceptible population $S_H(t)$ at a constant rate Λ_H. The susceptible humans either die at a natural death rate μ_H or move to the exposed class $E_H(t)$ due to infection caused by the cercariae $C(t)$ through skin penetration at a saturation rate $\lambda_H(t)$ (see Ref. 39) given by

$$\lambda_H(t) = \frac{\beta_H C(t)}{C_0 + C(t)}, \tag{2.1}$$

in which β_H is the maximal rate of exposure to cercariae and C_0 is the half saturation constant. The exposed humans do not immediately become infectious, but rather go through an incubation period for 4–8 weeks. During the incubation period, the exposed humans experience a local inflammatory response evidenced by a rash, called swimmer's itch. The exposed humans either die at a natural death rate μ_H,

or move to the infectious class I_H at a rate ψ_H. The infected humans die at a natural death rate μ_H, the additional disease induced death rate being denoted by δ_H and recovery rate of infected humans being given by κ_H. During the incubation period, the total cercariae population within an exposed human $C_H(t)$ is assumed to be removed through natural death at a constant rate μ_c or move to the lungs via blood vessels at a rate α_c, where it undergoes developmental changes to become immature worms denoted by $W_I(t)$. These immature worms are assumed to die by natural causes at a rate μ_I or migrate to the liver at a rate α_I. Due to further developmental changes, immature worms reach their sexual maturity, pair up and then migrate through the blood stream to their definitive locations. These occurrences are modeled by the ninth equation, the fraction $1/2$ capturing the pairing of immature worms. We denote the total population of mature worms within individuals by $W_m(t)$ and assume that mature worms die by natural causes at a rate μ_m or migrate to their definitive locations at a rate α_m. The total population of schistosome eggs $e_H(t)$ within infected humans appears since each worm pair lays an average of N_m eggs per day after having migrated to its definitive location at a rate α_m. We denote the rate at which the schistosome eggs die inside infected humans by μ_e and the rate at which they are excreted by the infected human hosts into the external environment by α_e, the excreted eggs then developing into free miracidia $M(t)$ at a net rate $N_e\alpha_e$. We assume that the free miracidia living in the external environment die by natural causes at a rate μ_p or infect susceptible vectors (snails) $S_v(t)$ at a rate $\lambda_v(t)$ (see Ref. 39), where

$$\lambda_v(t) = \frac{\beta_v M(t)}{M_0 + M(t)}. \tag{2.2}$$

In (2.2), β_v is the maximal rate of exposure to miracidia and M_0 is the half saturation constant.

The adult snails are recruited into the susceptible vector compartment at a constant rate Λ_v. Susceptible snails die by natural causes at a rate μ_v or move to the exposed vector compartment upon infection by miracidia. Exposed snails $E_v(t)$ die by natural causes at a rate μ_v, the additional parasite-induced death rate being denoted by δ_v. Due to the progression of the disease, the exposed snails proceed to the infectious compartment $I_v(t)$ at a rate ϕ_v. The infected snails die at a natural death rate μ_v, the additional parasite-induced death rate being also equal to δ_v. After 4–6 weeks, the infected snails begins to shed cercariae at a rate $N_s\gamma_s$, where N_s is the average number of cercariae shed by each snail per day and γ_s is the rate at which infected snails begin to shed cercariae. The cercariae population $C(t)$ in the external environment infects susceptible humans through skin penetration or die by natural causes at a rate μ_s.

To simplify our model, we have not considered the effect of the mating structure, although there is evidence of natural male bias in the sex ratio of *S. mansoni*,[45,46] being also determined that PZQ is more active against single male schistosoma, rather than against paired schistosomes.

On the basis of the above assumptions and remarks, one may construct the following model:

$$\begin{aligned}
\frac{dS_H}{dt} &= \Lambda_H - \lambda_H S_H - \mu_H S_H + \kappa_H I_H,\\
\frac{dE_H}{dt} &= \lambda_H S_H - (\mu_H + \psi_H) E_H,\\
\frac{dI_H}{dt} &= \psi_H E_H - (\mu_H + \delta_H + \kappa_H) I_H,\\
\frac{dS_v}{dt} &= \Lambda_v - \lambda_v S_v - \mu_v S_v,\\
\frac{dE_v}{dt} &= \lambda_v S_v - (\mu_v + \delta_v + \phi_v) E_v,\\
\frac{dI_v}{dt} &= \phi_v E_v - (\mu_v + \delta_v) I_v,\\
\frac{dC_H}{dt} &= (1-\tau)\omega\lambda_H S_H - (\alpha_c + \mu_c) C_H,\\
\frac{dW_I}{dt} &= \alpha_c C_H - (\alpha_I + \mu_I) W_I,\\
\frac{dW_m}{dt} &= \frac{\alpha_I}{2} W_I - (\alpha_m + \mu_m) W_m,\\
\frac{de_H}{dt} &= N_m \alpha_m W_m - (\alpha_e + \mu_e) e_H,\\
\frac{dM}{dt} &= N_e \alpha_e e_H - \mu_p M,\\
\frac{dC}{dt} &= N_s \gamma_s I_v - \mu_s C,
\end{aligned} \tag{2.3}$$

for which the state variables and parameter values are listed in Tables 1 to 4 and the flow diagram is given in Fig. 3.

Table 1. Description of all variables used for the model.

Description	Symbol
Size of the susceptible human population	$S_H(t)$
Size of the exposed human population	$E_H(t)$
Size of the infected human population	$I_H(t)$
Size of the susceptible snail population	$S_v(t)$
Size of the exposed snail population	$E_v(t)$
Size of the infected snail population	$I_v(t)$
Size of the cercariae population within exposed humans	$C_H(t)$
Size of the immature worms population within exposed humans	$W_I(t)$
Size of the mature worms population within exposed humans	$W_m(t)$
Number of worm eggs within infected humans	$e_H(t)$
Size of the miracidia population in the environment	$M(t)$
Size of the cercariae population in the environment	$C(t)$

Table 2. Description of variables and parameters used in the model. The time unit is per day.

Description	Symbol	Value	Range explored	Source
Recruitment rate of humans	Λ_H	800		37
Recruitment rate of vectors	Λ_v	3000		38
Humans progression rate from exposed to infected	ψ_H	0.017857	0.017857–0.023258	39
Recovery rate of infected humans	κ_H	0.0005567		19
Vector progression rate from exposed to infected	ϕ_v	0.034526	0.034526–0.0465	39
Disease induced death rate of humans	δ_H	0.00011	0.00002–0.00014	39
Natural death rate of humans	μ_H	0.0000438		48
Natural death rate of snails	μ_v	0.0029		36
Disease induced death rate of snails	δ_v	0.002		36
Maximum exposure rate of humans to cercariae	β_H	0.028		36
Maximum exposure rate of vectors to miracidia	β_v	0.000127		36
Migration rate of cercariae from skin to lungs	α_c	0.33	0.33–0.897	Estimated
Natural death rate of cercariae within exposed humans	μ_c	0.003	0.003–0.05	Estimated
Migration rate of immature worms from lungs to liver	α_I	0.0004	0.0004–0.0443	Estimated
Natural death rate of immature worms within exposed humans	μ_I	0.000456	0.000456–0.0014	17
Migration rate of mature worms from liver to definitive locations	α_m	0.0004	0.0004–0.4	Estimated
Natural death rate of mature worms within exposed humans	μ_m	0.000456	0.000456–0.0014	17
Number of eggs produced within exposed humans	N_m	300	300–3000	32

It is possible to prove via standard arguments that all solutions of the model (2.3) starting with positive initial data are positivity-preserving and eventually enter the invariant region:

$$\begin{aligned}\mathcal{D} = \{&(S_H, E_H, I_H, S_v, E_v, I_v, C_H, W_I, W_m, e_H, M, C) : 0 \le S_H, 0 \le E_H,\\ &0 \le I_H, S_H + E_H + I_H \le Q_1, 0 \le S_v, 0 \le E_v, 0 \le I_v, S_v + E_v + I_v \le Q_2,\\ &0 \le C_H \le Q_3, 0 \le W_I \le Q_4, 0 \le W_m \le Q_5, 0 \le e_H \le Q_6, 0 \le M \le Q_7,\\ &0 \le C \le Q_8\},\end{aligned}$$

where

$$Q_1 = \frac{\Lambda_H}{\mu_H},$$

$$Q_2 = \frac{\Lambda_v}{\mu_v},$$

$$Q_3 = \frac{(1-\tau)\omega}{\alpha_c + \mu_c} \cdot Q_9,$$

$$Q_4 = \frac{\alpha_c}{\alpha_I + \mu_I} \cdot \frac{1}{\alpha_c + \mu_c} \cdot Q_9,$$

$$Q_5 = \frac{\alpha_I}{\alpha_m + \mu_m} \cdot \frac{1}{2} \cdot \frac{\alpha_c}{\alpha_I + \mu_I} \cdot \frac{1}{\alpha_c + \mu_c} \cdot Q_9,$$

$$Q_6 = \frac{N_m \alpha_m}{\alpha_e + \mu_e} \cdot \frac{\alpha_I}{\alpha_m + \mu_m} \cdot \frac{1}{2} \cdot \frac{\alpha_c}{\alpha_I + \mu_I} \cdot \frac{1}{\alpha_c + \mu_c} \cdot Q_9,$$

$$Q_7 = \frac{N_e \alpha_e}{\mu_p} \cdot \frac{N_m \alpha_m}{\alpha_e + \mu_e} \cdot \frac{\alpha_I}{\alpha_m + \mu_m} \cdot \frac{1}{2} \cdot \frac{\alpha_c}{\alpha_I + \mu_I} \cdot \frac{1}{\alpha_c + \mu_c} \cdot Q_9,$$

$$Q_8 = \frac{N_s \gamma_s}{\mu_s} \cdot \frac{\Lambda_v}{\mu_v},$$

$$Q_9 = \frac{\beta_H \Lambda_H N_s \gamma_s \Lambda_v}{\mu_H C_0 \mu_s \mu_v + \mu_H N_s \gamma_s \Lambda_v}.$$

For the sake of brevity, we omit the proof here (see Ref. 47 for related arguments). We then conclude that the model (2.3) is epidemiologically feasible and mathematically well-posed in $\mathcal{D}$. In addition, the usual results on the existence, uniqueness and continuation of solutions also hold for (2.3).

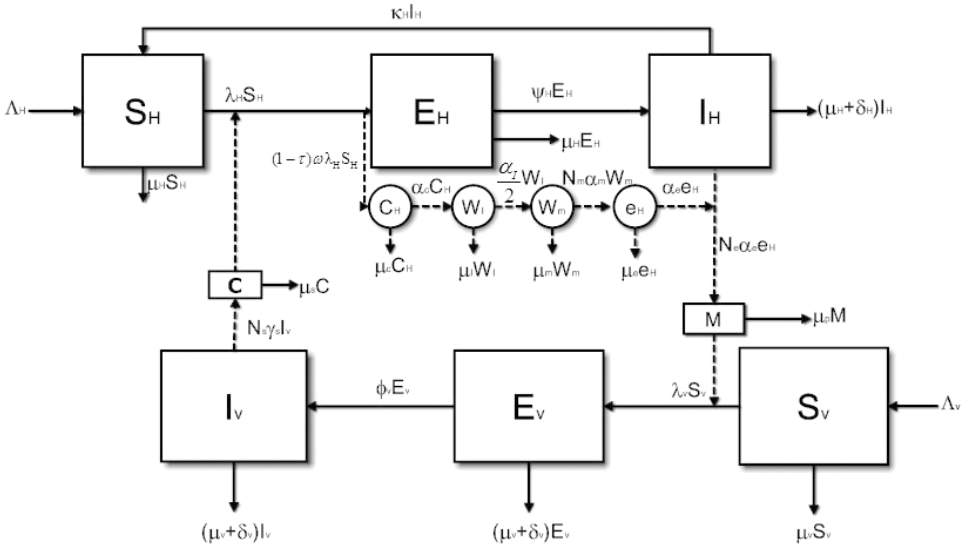

Fig. 3. A conceptual diagram of the mathematical model of human schistosomiasis, combining within-host and vector-host dynamics. The dashed arrows represent the schistosomiasis transmission within hosts and vectors, or between hosts and vectors, while solid arrows represent the progression of infection.

Table 3. Description of variables and parameters used in the model. The time unit is per day.

Description	Symbol	Values	Range explored	Source
Excretion rate of worm eggs into the environment	α_e	0.0004	0.0004–0.392	Estimated
Natural death rate of worm eggs	μ_e	0.0025	0.0025–0.25	12
Miracidia production rate per worm egg	N_e	0.01	0.006–0.02	18
Natural death rate of the miracidia	μ_p	2.526		36
Shedding rate of the cercariae by infected vector (snails)	γ_s	0.0182	0.0158–0.05	36
Natural death rate of the cercariae in the aquatic environment	μ_s	0.365		36
Amount of the cercariae shed by each snail	N_s	4128	3567–7895	36
Half saturation constant for the miracidia	M_0	10^8		38
Half saturation constant for the cercariae	C_0	9×10^6		38
Average cercariae uptake of an exposed individual	ω	1.06	1.02–4.02	Estimated
Decay parameter of the cercariae population	τ	$[0, 1]$		Estimated
Human progression rate from susceptible to exposed	λ_H			
Vector progression rate from susceptible to exposed	λ_v			

Table 4. Description of all variables from Ghana used for the model.

Description	Symbol	Values	Source
Initial size of the susceptible human population in Ghana	$S_H(0)$	20,000	23
Initial size of the exposed human population in Ghana	$E_H(0)$	200	58
Initial size of the infected human population in Ghana	$I_H(0)$	150	57
Recruitment rate of humans in Ghana	Λ_H	800	37
Natural death rate of humans in Ghana	μ_H	0.0000438	48

3. Model Analysis

3.1. *The disease-free equilibrium and its stability*

The system (2.3) has two equilibria, the disease-free equilibrium and the endemic equilibrium. At the disease-free equilibrium, there are no cercariae, miracidia, worms or eggs and hence there is no infection in either the human or the vector population. Thus, the model system (2.3) has a disease-free equilibrium E^0 given by

$$E^0 = \left(\frac{\Lambda_H}{\mu_H}, 0, 0, \frac{\Lambda_v}{\mu_v}, 0, 0, 0, 0, 0, 0, 0, 0\right). \tag{3.1}$$

Using the next generation method described in Ref. 50, it follows that the basic reproduction number of the system (2.3) is given by

$$R_0 = \sqrt{R_{0H} \cdot R_{0HS}}, \tag{3.2}$$

in which

$$R_{0H} = \frac{(1-\tau)\omega\beta_H\Lambda_H}{C_0\mu_H\mu_s} \cdot \frac{\alpha_c}{\alpha_c+\mu_c} \cdot \frac{\alpha_I}{\alpha_I+\mu_I} \cdot \frac{N_m\alpha_m}{\alpha_m+\mu_m} \cdot \frac{N_e\alpha_e}{\alpha_e+\mu_e} \cdot \frac{1}{2}$$

and

$$R_{0HS} = \frac{N_s\gamma_s\beta_v\Lambda_v\phi_v}{M_0\mu_v\mu_p(\mu_v+\delta_v)(\mu_v+\delta_v+\phi_v)}.$$

The quantity R_{0HS} has the following biological interpretation. Suppose that a single infected human is introduced into a completely susceptible snail population, then the average number of secondary snail infections that result from contact with the miracidia during the infectious period of the human is given by R_{0HS}.

Also, suppose that a single infected snail is introduced into a completely susceptible human population. Then, the average number of secondary human infections that result from contact with cercariae during the infectious period of the snail is given by R_{0H}.

Furthermore, we deduce that the snail to human transmission coefficient R_{0H} is a product of two other transmission coefficients which are the vector-host (snail to human) transmission coefficient R_{0SH} and the within-host transmission (within-human) R_{0WH} which are given by

$$R_{0H} = R_{0SH} \cdot R_{0WH},$$

where

$$R_{0SH} = \frac{(1-\tau)\omega\beta_H\Lambda_H}{C_0\mu_H\mu_s}$$

and

$$R_{0WH} = \frac{\alpha_c}{\alpha_c+\mu_c} \cdot \frac{\alpha_I}{\alpha_I+\mu_I} \cdot \frac{N_m\alpha_m}{\alpha_m+\mu_m} \cdot \frac{N_e\alpha_e}{\alpha_e+\mu_e} \cdot \frac{1}{2}.$$

Hence, the basic reproduction number R_0 can be computed as

$$R_0 = \sqrt{R_{0WH} \cdot R_{0SH} \cdot R_{0HS}},$$

keeping track of both vector-host and within-host disease parameters, R_{0HS}, R_{0SH} and R_{0WH}, respectively.

From the expression of R_0, the following deductions are made:

- Reducing the contact of humans with infested cercariae waters through the provisioning of safe drinking water and hygiene education may lead to the control of the disease via a reduction of the maximum exposure rate of humans to cercariae β_H.
- The natural death rate of the cercariae in the aquatic environment μ_s and the natural death rate of miracidia μ_p have a significant impact on the disease transmission. This suggests that control measures cause an increase in the death rate of cercariae and miracidia may also lead to the control of the disease.

- Within host disease parameters such as the penetration rate of cercariae ω, the migration rate of cercariae from skin to lungs α_c, the number of eggs produced within an exposed human N_m, the migration rate of immature worms from lungs to liver α_I and the migration rate of mature worms from liver to definitive locations α_m contribute significantly to disease transmission and prevalence. This suggests that effective drugs that can reduce those parameters will facilitate the control of the disease.

From Theorem 2 of Ref. 50, the following stability result is obtained.

Theorem 3.1. *The disease-free equilibrium* E^0 *of* (2.3) *is locally asymptotically stable if* $R_0 < 1$ *and unstable if* $R_0 > 1$, *where* R_0 *is given by* (3.2).

3.2. *The existence of the endemic equilibrium*

At the endemic equilibrium, the vectors (snails) are infected with miracidia and humans are infected with cercariae. The coordinates of the endemic equilibrium

$$E^* = (S_H^*, E_H^*, I_H^*, S_v^*, E_v^*, I_v^*, C_H^*, W_I^*, W_m^*, e_H^*, M^*, C^*)$$

verify the equilibrium relations

$$\lambda_H^* S_H^* = \Lambda_H - \mu_H S_H^* + \kappa_H I_H^*, \tag{3.3}$$

$$S_H^* = \frac{(\mu_H + \psi_H) E_H^*}{\lambda_H^*}, \tag{3.4}$$

$$E_H^* = \frac{(\mu_H + \delta_H + \kappa_H) I_H^*}{\psi_H}, \tag{3.5}$$

$$S_v^* = \frac{\Lambda_v}{\lambda_v^* + \mu_v}, \tag{3.6}$$

$$E_v^* = \frac{\lambda_v^* S_v^*}{\mu_v + \delta_v + \phi_v}, \tag{3.7}$$

$$E_v^* = \frac{(\mu_v + \delta_v) I_v^*}{\phi_v}, \tag{3.8}$$

$$C_H^* = \frac{(1-\tau)\omega \lambda_H^* S_H^*}{\alpha_c + \mu_c}, \tag{3.9}$$

$$W_I^* = \frac{\alpha_c C_H^*}{\alpha_I + \mu_I}, \tag{3.10}$$

$$W_m^* = \frac{\alpha_I W_I^*}{\alpha_m + \mu_m} \cdot \frac{1}{2}, \tag{3.11}$$

$$e_H^* = \frac{N_m \alpha_m W_m^*}{\alpha_e + \mu_e}, \tag{3.12}$$

$$M^* = \frac{N_e \alpha_e e_H^*}{\mu_p}, \tag{3.13}$$

$$I_v^* = \frac{\mu_s C^*}{N_s \gamma_s}, \tag{3.14}$$

where λ_H^* and λ_v^* are given by

$$\lambda_H^* = \frac{\beta_H C^*}{C_0 + C^*}, \tag{3.15}$$

$$\lambda_v^* = \frac{\beta_v M^*}{M_0 + M^*}. \tag{3.16}$$

We may now obtain the following existence and uniqueness result, whose proof is given in Appendix A.

Theorem 3.2. *The system* (2.3) *has a unique endemic equilibrium*

$$E^* = (S_H^*, E_H^*, I_H^*, S_v^*, E_v^*, I_v^*, C_H^*, W_I^*, W_m^*, e_H^*, M^*, C^*)$$

if and only if $R_0 > 1$.

3.3. *Local stability of the endemic equilibrium*

Computing the eigenvalues of the Jacobian matrix of (2.3) at the endemic equilibrium is very tedious. Instead, we employ the approach of Ref. 51 and analyze the bifurcation of the solutions of (2.3) at the disease-free equilibrium by using the Center Manifold Theorem. We make the following notations in (2.3):

$$x_1 = S_H, x_2 = E_H, x_3 = I_H, x_4 = S_v, x_5 = E_v, x_6 = I_v,$$

$$x_7 = C_H, x_8 = W_I, x_9 = W_m, x_{10} = e_H, x_{11} = M, x_{12} = C.$$

The model system (2.3) is then written in vector form as

$$\frac{dX}{dt} = H(X), \tag{3.17}$$

in which $X = (x_1, x_2, x_3, \ldots, x_{12})^T$ and $H = (h_1, h_2, h_3, \ldots, h_{12})^T$.

Suppose that $\beta_v = g\beta_H$ and let β_H be the bifurcation parameter. Solving the equation $R_0 = 1$ gives us $\beta_H = \beta^*$, with

$$\beta^* = \sqrt{\frac{2C_0\mu_H\mu_s(\mu_v + \delta_v)\mu_v M_0 \mu_p(\mu_v + \delta_v + \phi_v)(\alpha_c + \mu_c) \times (\alpha_I + \mu_I)(\alpha_m + \mu_m)(\alpha_e + \mu_e)}{(1-\tau)\omega\Lambda_H N_s\gamma_s g\Lambda_v\phi_v\alpha_c\alpha_I N_m\alpha_m N_e\alpha_e}}.$$

The following result, whose proof is given in Appendix B, characterizes the stability of E^* for values of R_0 which are larger than 1, but close to 1.

Theorem 3.3. *The unique endemic equilibrium* E^* *is locally asymptotically stable for* $R_0 > 1$, *but close to* 1.

4. A Sensitivity Analysis of R_0

In what follows, we shall investigate how R_0 responds to changes in the parameters, in order to determine the parameters whose changes have the highest impact on R_0 and have the potential to lead to effective control and elimination of the disease. The normalized forward-sensitivity index of a variable Q with respect to a parameter p (or the elasticity of Q with respect to p) is defined as

$$\Upsilon_p^Q = \frac{p}{Q} \cdot \frac{\partial Q}{\partial p}.$$

This index indicates how sensitive Q is to changes of parameter p. Precisely, a positive (negative) index indicates that an increase in the parameter value results in an increase (decrease) of Q.[52,53]

We derive the sensitivity of R_0 to each of the 29 within-host and vector-host parameters described (See also Appendix C). From Fig. 4, R_0 is most sensitive to μ_v the natural death rate of vectors, followed by $(N_s, \gamma_s, N_m, \beta_v, \beta_H, \Lambda_H, \Lambda_v)$ and $(\mu_m, \mu_H, \mu_p, \mu_s, \mu_e)$. Also, R_0 is least sensitive to δ_H, the disease induced death rate of humans and to δ_v, the disease induced death rate of vectors.

One sees that $\Upsilon_{\mu_v}^{R_0} = -2$, which means that increasing or (decreasing) μ_v the natural death rate of the vector by 10%, decreases or (increases) R_0 by 20%. Similarly, the normalized sensitivity indices for all parameters in $(\mu_m, \mu_H, \mu_p, \mu_s, \mu_e)$ are equal to -1, which means that increasing or (decreasing) these parameters $(\mu_m, \mu_H, \mu_p, \mu_s, \mu_e)$ by 10%, decreases or (increases) R_0 by 10%. Furthermore, the sensitivity indices for all parameters in $(N_s, \gamma_s, N_m, \beta_v, \beta_H, \Lambda_H, \Lambda_v)$ are equal to 1, this implies that increasing or (decreasing) these parameters by 10% increases (decreases) R_0 by 10%.

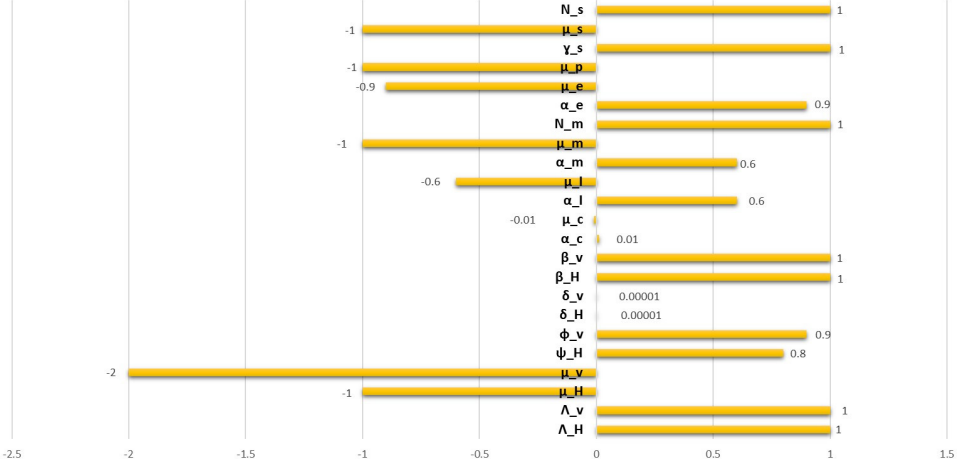

Fig. 4. Sensitivity indices for R_0 against model parameters.

The above remarks suggest that control strategies that effectively reduce the natural death rate of vectors μ_v, the number of cercariae shed by each snail per day N_s, the shedding rate γ_s of cercariae by infected vector (snail), the number of eggs produced within the exposed human N_m, the maximum exposure rate β_v of vector to miracidia, the maximum exposure β_H of humans to cercariae should be used to control the disease transmission effectively. Also, increases in cercariae death rate, miracidia death rate, mature worm death rate and worm eggs death rate will all lead to a corresponding decrease in R_0, hence all control strategies to reduce the transmission of schistosomiasis effectively must strive for achieving higher death rates of worm eggs μ_e, mature worm eggs μ_m, miracidia μ_p and cercariae μ_s. Hence, from a mathematical viewpoint, these strategies are u_1 (access to safe water, improved sanitation and hygiene education), u_2 (large-scale treatment of infected population groups) and u_3 (reducing the vector (snail) population by the use of molluscicides), which would be specified in our following model.

5. Optimal Control Strategies

In this section, we extend our model (2.3) by introducing three time-dependent control measures, namely $u_1(t)$ (access to safe water, improved sanitation and hygiene education), $u_2(t)$ (large-scale treatment of infected population groups) and $u_3(t)$ (reducing the vector (snail) population by the use of molluscicides) to curtail the spread of schistosomiasis. It is assumed that in the human population, the associated force of infection is reduced by a factor of $1/(1+u_1(t))$, as more susceptible humans gain access to safe water, improved sanitation and hygiene education. Furthermore, the disease induced death rate is reduced by a factor of $1/(1+u_2(t))$ as more infected humans are treated. The reproduction rate of the vector (snail) population is also reduced by a factor of $1/(1+u_3(t))$ as more snails are removed.

The model system (2.3) becomes

$$\begin{aligned}
\frac{dS_H}{dt} &= \Lambda_H - \frac{\lambda_H S_H}{1+u_1(t)} - \mu_H S_H + \kappa_H I_H,\\
\frac{dE_H}{dt} &= \frac{\lambda_H S_H}{1+u_1(t)} - (\mu_H + \psi_H) E_H,\\
\frac{dI_H}{dt} &= \psi_H E_H - (\mu_H + \frac{\delta_H}{1+u_2(t)}) I_H - \kappa_H I_H,\\
\frac{dS_v}{dt} &= \frac{\Lambda_v}{1+u_3(t)} - \lambda_v S_v - \mu_v S_v,\\
\frac{dE_v}{dt} &= \lambda_v S_v - (\mu_v + \delta_v) E_v - \phi_v E_v,\\
\frac{dI_v}{dt} &= \phi_v E_v - (\mu_v + \delta_v) I_v,
\end{aligned}$$

$$\begin{aligned}
\frac{dC_H}{dt} &= \frac{(1-\tau)\omega\lambda_H S_H}{1+u_1(t)} - (\alpha_c+\mu_c)C_H,\\
\frac{dW_I}{dt} &= \alpha_c C_H - (\alpha_I+\mu_I)W_I,\\
\frac{dW_m}{dt} &= \frac{\alpha_I}{2}W_I - (\alpha_m+\mu_m)W_m,\\
\frac{de_H}{dt} &= N_m\alpha_m W_m - (\alpha_e+\mu_e)e_H,\\
\frac{dM}{dt} &= N_e\alpha_e e_H - \mu_p M,\\
\frac{dC}{dt} &= N_s\gamma_s I_v - \mu_s C,
\end{aligned} \tag{5.1}$$

with the given objective function

$$J(u_1,u_2,u_3) = \int_0^T [c_1 I_H + c_2 N_v + c_3 u_1^2 + c_4 u_2^2 + c_5 u_3^2]dt, \tag{5.2}$$

where N_v is the total vector population, T is the final time and the coefficients c_1, c_2, c_3, c_4, c_5 are positive weights. Our aim is to minimize the total number of infected humans and the snail population while minimizing the cost of control $u_1(t), u_2(t), u_3(t)$. Thus, we search for an optimal control u_1^*, u_2^*, u_3^* such that

$$J(u_1^*,u_2^*,u_3^*) = \min_{u_1,\ u_2,\ u_3}\{J(u_1,u_2,u_3)\,|\,u_1,u_2,u_3\in\Omega\}, \tag{5.3}$$

where the control set is

$$\Omega = \{(u_1,u_2,u_3)\,|\,u_i:[0,T]\to[0,\infty) \text{ Lebesgue measurable},\ i=1,2,3\}.$$

The terms $c_1 I_H$ and $c_2 N_v$ represent the cost of infection and cost of reducing the vector population, respectively, while $c_3 u_1^2$ is the cost of access to safe water, improved sanitation and hygiene education. Also, $c_4 u_2^2$ is the cost of large-scale treatment of infected population groups and $c_5 u_3^2$ is the cost of reducing the vector (snail) population by the use of molluscicides. The necessary conditions that an optimal control must satisfy come from the Pontryagin's Minimum Principle.[41] This principle converts Eqs. (5.1) and (5.2) into a problem of point-wise minimizing a Hamiltonian H with respect to (u_1,u_2,u_3).

$$\begin{aligned}
H &= c_1 I_H + c_2 N_v + c_3 u_1^2 + c_4 u_2^2 + c_5 u_3^2\\
&\quad + \lambda_{S_H}\left\{\Lambda_H - \frac{\lambda_H S_H}{(1+u_1(t))} - \mu_H S_H + \kappa_H I_H\right\}\\
&\quad + \lambda_{E_H}\left\{\frac{\lambda_H S_H}{(1+u_1(t))} - (\mu_H+\psi_H)E_H\right\}\\
&\quad + \lambda_{I_H}\left\{\psi_H E_H - \left(\mu_H + \frac{\delta_H}{(1+u_2(t))}\right)I_H - \kappa_H I_H\right\}
\end{aligned}$$

$$
\begin{aligned}
&+\lambda_{S_v}\left\{\frac{\Lambda_v}{(1+u_3(t))}-\lambda_v S_v-\mu_v S_v\right\}\\
&+\lambda_{E_v}\{\lambda_v S_v-(\mu_v+\delta_v)E_v-\phi_v E_v\}\\
&+\lambda_{I_v}\{\phi_v E_v-(\mu_v+\delta_v)I_v\}+\lambda_{C_H}\left\{\frac{(1-\tau)\omega\lambda_H S_H}{(1+u_1(t))}-(\alpha_c+\mu_c)C_H\right\}\\
&+\lambda_{W_I}\{\alpha_c C_H-(\alpha_I+\mu_I)W_I\}+\lambda_{W_m}\left\{\frac{\alpha_I}{2}W_I-(\alpha_m+\mu_m)W_m\right\}\\
&+\lambda_{e_H}\{N_m\alpha_m W_m-(\alpha_e+\mu_e)e_H\}\\
&+\lambda_M\{N_e\alpha_e e_H-\mu_p M\}\\
&+\lambda_C\{N_s\gamma_s I_v-\mu_s C\},
\end{aligned}
$$

where λ_{S_H}, λ_{E_H}, λ_{I_H}, λ_{I_H}, λ_{S_v}, λ_{E_v}, λ_{I_v} λ_{C_H}, λ_{W_I}, λ_{W_m}, λ_{e_H}, λ_M and λ_C are the adjoint variables or co-state variables.[41]

$$
\begin{aligned}
-\frac{d\lambda_{S_H}}{dt}&=\frac{\partial H}{\partial S_H}=-\left[\frac{\lambda_H}{(1+u_1(t))}+\mu_H\right]\lambda_{S_H}+\frac{\lambda_H}{(1+u_1(t))}\lambda_{E_H}\\
&\quad+\frac{(1-\tau)\omega\lambda_H}{(1+u_1(t))}\lambda_{C_H},\\
-\frac{d\lambda_{E_H}}{dt}&=\frac{\partial H}{\partial E_H}=-(\mu_H+\psi_H)\lambda_{E_H}+\psi_H\lambda_{I_H},\\
-\frac{d\lambda_{I_H}}{dt}&=\frac{\partial H}{\partial I_H}=c_1+\kappa_H\lambda_{S_H}-\left[\mu_H+\frac{\delta_H}{(1+u_2(t))}+\kappa_H\right]\lambda_{I_H},\\
-\frac{d\lambda_{S_v}}{dt}&=\frac{\partial H}{\partial S_v}=c_2-[\lambda_v+\mu_v]\lambda_{S_v}+\lambda_v\lambda_{E_v},\\
-\frac{d\lambda_{E_v}}{dt}&=\frac{\partial H}{\partial E_v}=c_2-[(\mu_v+\delta_v)+\phi_v]\lambda_{E_v}+\phi_v\lambda_{I_v},\\
-\frac{d\lambda_{I_v}}{dt}&=\frac{\partial H}{\partial I_v}=c_2-[(\mu_v+\delta_v)]\lambda_{I_v}+N_s\gamma_s\lambda_C,\\
-\frac{d\lambda_{C_H}}{dt}&=\frac{\partial H}{\partial C_H}=-(\alpha_c+\mu_c)\lambda_{C_H}+\alpha_c\lambda_{W_I},\\
-\frac{d\lambda_{W_I}}{dt}&=\frac{\partial H}{\partial W_I}=-(\alpha_I+\mu_I)\lambda_{W_I}+\frac{\alpha_I}{2}\lambda_{W_m},\\
-\frac{d\lambda_{W_m}}{dt}&=\frac{\partial H}{\partial W_m}=-(\alpha_m+\mu_m)\lambda_{W_m}+N_m\alpha_m\lambda_{e_H},\\
-\frac{d\lambda_{e_H}}{dt}&=\frac{\partial H}{\partial e_H}=-(\alpha_e+\mu_e)\lambda_{e_H}+N_e\alpha_e\lambda_M,
\end{aligned}
$$

$$-\frac{d\lambda_M}{dt} = \frac{\partial H}{\partial M} = \frac{\beta_v M_0 S_v}{(M_0+M)^2}(\lambda_{E_v} - \lambda_{S_v}) - \mu_p \lambda_M,$$

$$-\frac{d\lambda_C}{dt} = \frac{\partial H}{\partial C} = \frac{\beta_H C_0 S_H}{(C_0+C)^2(1+u_1(t))}(\lambda_{E_H} - \lambda_{S_H}) + \frac{(1-\tau)\omega\beta_H C_0 S_H}{(C_0+C)^2(1+u_1(t))}\lambda_{C_H} - \mu_s \lambda_C.$$

The transversality conditions are

$$\lambda_{S_H}(T) = \lambda_{E_H}(T) = \lambda_{I_H}(T) = \lambda_{S_v}(T) = \lambda_{E_v}(T) = \lambda_{I_v}(T) = \lambda_{C_H}(T) = \lambda_{W_I}(T) = \lambda_{W_m}(T) = \lambda_{e_H}(T) = \lambda_M(T) = \lambda_C(T) = 0.$$

On the interior of the control set, where $0 < u_i < 1$, for $i = 1, 2, 3$, we have

$$\frac{\partial H}{\partial u_1} = 2c_3 u_1 + \left(\frac{\lambda_H S_H}{(1+u_1(t))^2}\right)(\lambda_{S_H} - \lambda_{E_H}) - \left(\frac{(1-\tau)\omega\lambda_H S_H}{(1+u_1(t))^2}\right)\lambda_{C_H}$$

$$\frac{\partial H}{\partial u_2} = 2c_4 u_2 + \left(\frac{\delta_H I_H}{(1+u_2(t))^2}\right)\lambda_{I_H} = 0,$$

$$\frac{\partial H}{\partial u_3} = 2c_5 u_3 - \left(\frac{\Lambda_v}{(1+u_3(t))^2}\right)\lambda_{S_v} = 0.$$

Let $A = \lambda_H S_H(\lambda_{S_H} - \lambda_{E_H} - (1-\tau)\omega\lambda_{C_H})$ and $B = \delta_H I_H \lambda_{I_H}$.
We then obtain that

$$u_1 = 1/6\,\frac{\sqrt[3]{(6\sqrt{3}\sqrt{A(27A-8c_3)}-54A+8c_3){c_3}^2}}{c_3} + 2/3\,\frac{c_3}{\sqrt[3]{(6\sqrt{3}\sqrt{A(27A-8c_3)}-54A+8c_3){c_3}^2}} - 2/3,$$

$$u_2 = 1/6\,\frac{\sqrt[3]{(6\sqrt{3}\sqrt{B(27B-8c_4)}-54B+8c_4){c_4}^2}}{c_4} + 2/3\,\frac{c_4}{\sqrt[3]{(6\sqrt{3}\sqrt{B(27B-8c_4)}-54B+8c_4){c_4}^2}} - 2/3,$$

$$u_3 = 1/6\,\frac{\sqrt[3]{(6\sqrt{3}\sqrt{\Lambda_v(27\Lambda_v+8c_5)}+54\Lambda_v+8c_5){c_5}^2}}{c_5} + 2/3\,\frac{c_5}{\sqrt[3]{(6\sqrt{3}\sqrt{\Lambda_v(27\Lambda_v+8c_5)}+54\Lambda_v+8c_5){c_5}^2}} - 2/3.$$

Finally, since in our problem there are no terminal values for the state variables, we give transversality conditions at the final time T by

$$\lambda_i(T) = 0, i = 1, 2, 3.$$

6. Numerical Simulations

In this section, we investigate, from a numerical viewpoint, the effects of the optimal control strategies on the spread of schistosomiasis in the Ghanaian population. The optimal control is determined by solving the optimality system, consisting of 12 ordinary differential equations and representing the state and adjoint equations. The numerical approach deals with a two-point boundary value problem with the boundary conditions at $t = 0$ and $t = T$ by using the Matlab package bvp4c.

Using an integrated control approach which combines all three control measures at the same time, we investigate and compare the corresponding results of the numerical simulations. For the numerical simulations, we choose values for the variables and parameters based on available references, as shown in Tables 2 to 4 above. The other values are estimated or assumed based on data from Ghana health service. Also, to illustrate the effect of integrated optimal control strategies on the spread of schistosomiasis in the population, we use the following weight factors: $c_1 = 90$, $c_2 = 50$, $c_3 = 60$, $c_4 = 40$ and $c_5 = 35$, for which the basic reproduction number takes the value $R_0 = 3.0308$. Thus, we have considered the spread of schistosomiasis in an endemic population, as it should be the case in a real-life scenario. The optimal strategy integrates all three control measures and applies them simultaneously to control the disease. The optimal control profiles are given in Fig. 6.

6.1. *The effects of optimal integrated controls on the susceptible human population*

Figure 5(a) shows a substantial difference in the sizes of the susceptible human population with and without using controls. Without using controls, the size of

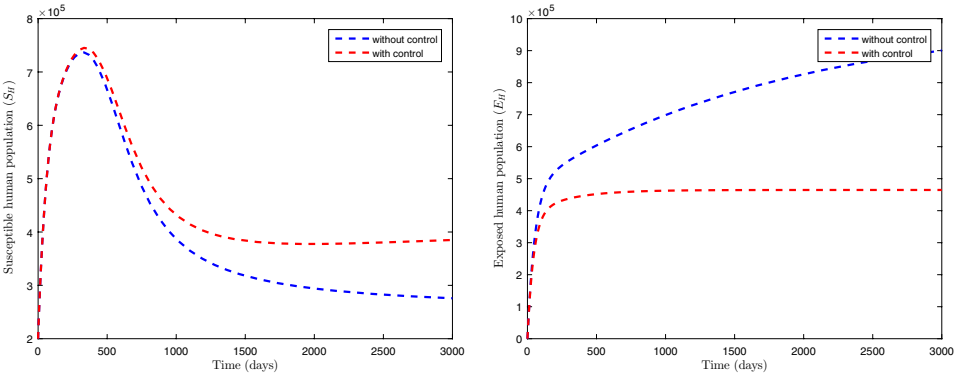

(a) (b)

Fig. 5. Simulations showing the effect of u_1 (access to safe water, improved sanitation and hygiene education), u_2 (large-scale treatment of infected population groups) and u_3 (reducing the vector (snail) population by the use of molluscicides) on (a) susceptible human populations, (b) exposed human populations, (c) infected human populations, (d) infected vector populations.

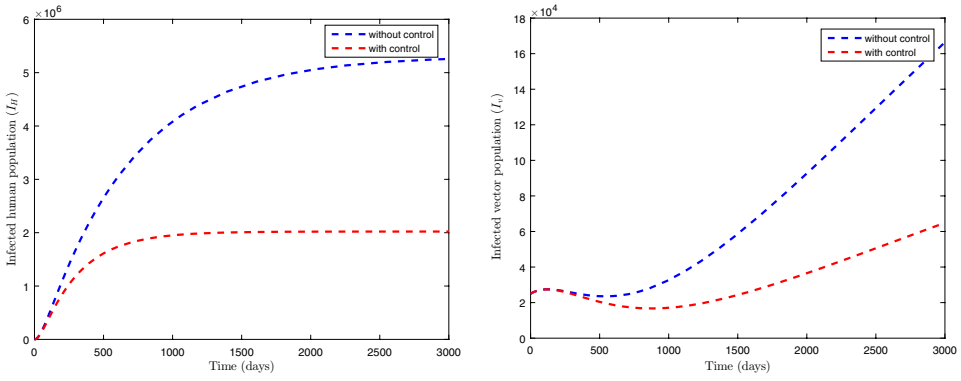

(c) (d)

Fig. 5. (*Continued*)

susceptible human population decreases faster and reaches a lower peak, while in the controlled case, the size of the of susceptible human population decreases at a slower rate compared and reaches a higher peak. This suggests that more humans were transferred into the exposed compartment in the uncontrolled case.

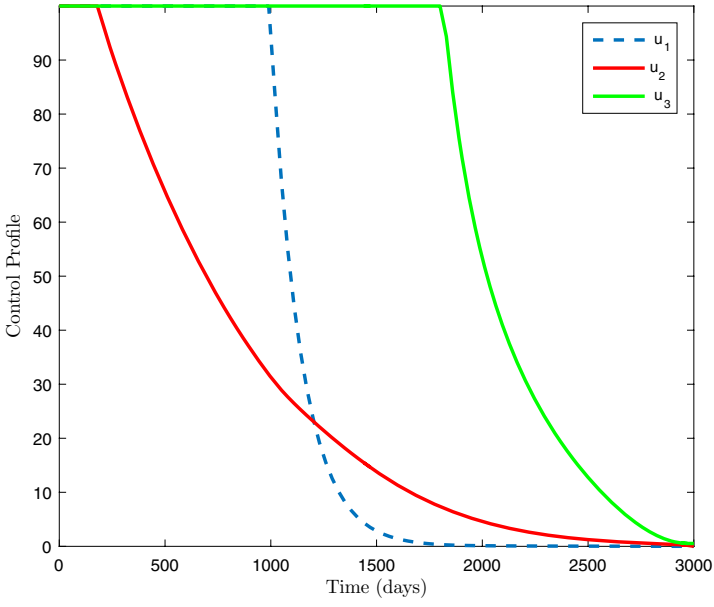

Fig. 6. Simulation showing the optimal control profile of u_1,u_2 and u_3. Blue dash lines: control profile of access to safe water, improved sanitation and hygiene education, red solid line: control profile of large-scale treatment of infected population groups and green solid line: control profile of reducing the vector (snail) population by the use of molluscicides.

6.2. *The effects of optimal integrated controls on the exposed human population*

As shown in Figure 5(b), the size of the exposed human population decreases rapidly under the integrated optimal control strategy, compared to what happens in the uncontrolled case. This suggests that under integrated optimal control strategies, the prevalence of schistosomiasis will be kept at very low levels.

6.3. *The effects of optimal integrated controls on the infected human population*

Again, as seen in Fig. 5(c), the size of the infected human population decreases rapidly under the integrated optimal control strategy, compared to what happens in the uncontrolled case. This further suggests that under integrated optimal control strategies, very few humans will be infected with the disease and prevalence of schistosomiasis will be kept at very low levels.

7. Conclusions

In this paper, a 12-dimensional system of ordinary differential equations describing both within-host and vector-host dynamics is formulated to describe the transmission of schistosomiasis. This model is then analyzed using stability theory, optimal control theory and numerical simulations. By using the next generation method proposed in Ref. 49 and the approach in Ref. 50, an explicit expression for the basic reproduction number R_0 is derived and interpreted from a biological viewpoint. It is determined that both within-host and vector-host parameters contribute to R_0, which suggests that both environmental factors and human immune system factors contribute to the transmission of schistosomiasis.

The stability analysis of the 12-dimensional nonlinear system is investigated with respect to the values of R_0. It is observed that if $R_0 < 1$, then the disease free equilibrium is locally asymptotically stable, while the system has a single positive equilibrium provided that $R_0 > 1$. For $R_0 > 1$, the local stability of the unique positive equilibrium is investigated using the Center Manifold Theorem proposed in Ref. 51, being determined that the unique endemic equilibrium is locally asymptotically stable for $R_0 > 1$, but near 1.

A sensitivity analysis indicates that R_0 is sensitive to both within-host and vector-host parameters, R_0 being most sensitive to the natural death rate of vector population μ_v. This suggests that periodic harvesting and removal of the vector population should be done to control the spread of the disease. The basic reproduction number obtained for the model is 3.0308, confirming the fact that schistosomiasis is endemic in Ghana, as stated in Ref. 22.

Furthermore, optimal control theory is applied to investigate the corresponding optimal control problem. By using the Pontryagin's Minimum Principle necessary conditions are provided for the existence of the optimal solution to the optimal

control problem. Finally, numerical simulations are presented to verify the theoretical results, to assess the effectiveness and impact of integrated control on schistosomiasis transmission.

The numerical simulations indicate that the size of the infected population decreased considerably in the controlled case. This suggests that a future free from schistosomiasis can be achieved in Ghana if all three control measures u_1 (access to safe water, improved sanitation and hygiene education), u_2 (large-scale treatment of infected population groups) and u_3 (reducing the vector (snail) population by the use of molluscicides) are implemented at the same time for a significant amount of time. We suggest that mass drug administration of PZQ should be done together with periodic harvesting and killing of the vector (snail) population and educating the public to avoid contact with infected water bodies containing cercariae. Therefore a clean environment, strong protective human immune system with reduced vector (snail) population will lead to a minimal transmission of schistosomiasis and flatworm diseases in Ghana.

As noted in Ref. 54, the reliance of schistosomiasis control programmes upon the use of a small number of drugs makes those control measures vulnerable to the emergence of drug resistance. Although there is no evidence of established, systematic resistance to PZQ, even with the widespread and continuous, long-term use of this drug, there are occasional reports of individual PZQ treatment failures for travelers with schistosomiasis.[55]

Consequently, while our model does not allow for dynamic features, it is important to consider, as an avenue of further research, the impact of drug resistance induced by mass chemotherapy and of host-parasite coevolution. A systematic study in the latter direction, from an experimental viewpoint, has been performed in Refs. 54 and 56 observing that drug resistant parasites may incur adaptation costs, such as a lower reproduction rate, especially since the schistosomes are required to adapt to both their intermediate and definitive hosts.

The impact of host-parasite coevolution on the definitive hosts (humans) remains difficult to assess, due to the ethical aspects involved in performing controlled experiments. The intermediate hosts (snails) present, in this regard, a much better opportunity to investigate the outcome of coevolution. It has been observed in Ref. 56 that, from the viewpoint of the intermediate host, resistance is dominant over susceptibility, being also a heritable trait, while the resistance phenotype may be simultaneously displayed against multiple parasite strains, features which suggest that resistance is a multilocus trait.

A sensitivity analysis meant to predict the impact of long-term temperature changes upon the prevalence of schistosomiasis, as quantified by the mean worm burden of a human host, and upon the choice of an appropriate control strategy has been performed in Ref. 36. While our results are not directly comparable with those obtained in Ref. 36, since our concern here is incidence, not prevalence, and the human population is considered to be at equilibrium therein, the model under investigation involving life stages for snails instead, there are common conclusions,

amounting to the fact that the natural mortality rate of snails ranks highly, if not the highest, on the list of most sensitive parameters. Also, the disease-induced mortality rate of snails ranks is comparatively low on the same list, and, even though the mean worm burden may increase as high as 10-fold, as seen in Ref. 36, the size of the infected population is unlikely to change greatly under most common circumstances.

Our model is only a crude approximation of reality, certain simplifications being made for the sake of simplicity and tractability. In particular, as suggested by one of the referees, there should be more impact of the within-host and vector–host interactions on each other (for instance, the disease-induced death rate of the host should depend on the parasite load). Although this is highly desirable, since it greatly improves the accuracy of the model and, due to the stronger coupling of the sub-models, it has the potential to elicit richer dynamics, it also vastly diminishes the chances of obtaining explicit and easily interpretable expressions of $\mathcal{R}_0$, due to the subsequent changes in the structure of the next generation matrix and vastly complicates the discussion on the existence and properties of the endemic equilibrium. Improving the connection between within-host and vector-host modeling remains, however, an avenue of further research.

Acknowledgments

We thank the Managing Editors and two anonymous reviewers for their constructive comments, which helped us to improve the manuscript, both in content and in its presentation. The work of PG was supported by a grant of the Romanian National Authority for Scientific Research, CNCS-UEFISCDI, project number PN-II-ID-PCE-2011-3-0557.

References

1. Stroehlein AJ, Young ND, Jex AR, Sternberg PW, Tan P, Boag PR, Hofmann A, Gasser RB, Defining the Schistosoma haematobium kinome enables the prediction of essential kinases as anti-schistosome drug targets, *Sci Rep* **5**:17759, 2015, doi: 10.1038/srep17759.
2. World Health Organization, Schistosomiasis fact sheet, Available at http://www.who.int/mediacentre/factsheets/fs115/en/ (accessed August 2017).
3. World Health Organization, Schistosomiasis Progress Report (2001–2011) and Strategic Plan (2012–2020), World Health Organization Press, Geneva, Switzerland, 2013, Available at http://www.who.int/schistosomiasis/resources/en/ (accessed April 2016).
4. World Health Organization, The global burden of disease: 2004 update, World Health Organization Press, Geneva, Switzerland, 2008, Available at http://www.who.int/healthinfo/global_burden_disease/2004_report_update/en/ (accessed August 2017).
5. King CH, Parasites and poverty: the case of schistosomiasis, *Acta Trop* **113**(2):95–104, 2010.
6. Gryseels B, Polman K, Clerinx J, Kestens L, Human schistosomiasis, *Lancet* **368**(9541):1106–1118, 2006.

7. Barry MA, Simon GG, Mistry N, Hotez PJ, Global trends in neglected tropical disease control and elimination: impact on child health, *Arch Dis Child* **98**(8):635–641, 2013.
8. Gryseels B, Strickland GM, Schistosomiasis, in Magill AJ, Hill DR, Solomon T, Ryan ET (eds.), *Hunter's Tropical Medicine and Emerging Infectious Disease*, 9th edn., Elsevier, Philadelphia, 2013.
9. Ross AG, Vickers D, Olds GR, Shah SM, McManus DP, Human schistosomiasis, *Lancet Infect Dis* **7**(3):218–224, 2007.
10. Gryseels B, Schistosomiasis, *Infect Dis Clin North Am* **26**(2):383–397, 2012.
11. Curwen RS, Wilson RA, Invasion of skin by schistosome cercariae: some neglected facts, *Trends Parasitol* **19**(2):63–66, 2003.
12. Hammam OA, Elkhafif N, Attia YM, Mansour MT, Elmazar MM, Abdelsalam RM, Kenawy SA, El-Khatib AS, Wharton's jelly-derived mesenchymal stem cells combined with praziquantel as a potential therapy for Schistosoma mansoni-induced liver fibrosis, *Sci Rep* **6**:21005, 2016, doi: 10.1038/srep21005.
13. Hagen J, Young ND, Every AL, Pagel CN, Schnoeller C, Scheerlinck JPY, Gasser RB, Kalinna BH, Omega-1 knockdown in Schistosoma mansoni eggs by lentivirus transduction reduces granuloma size in vivo, *Nat Commun* **5**:5375, 2014, doi: 10.1038/ncomms6375.
14. Nascimento-Carvalho VM, Moreno-Carvalho OA, Neuroschistosomiasis due to Schistosoma mansoni: a review of pathogenesis, clinical syndromes and diagnostic approaches, *Rev Inst Med Trop Sao Paulo* **47**(4):179–184, 2005.
15. Mathers CD, Ezzati M, Lopez AD, Measuring the burden of neglected tropical diseases: the global burden of disease framework, *PLoS Negl Trop Dis* **71**(2):e114, 2007.
16. Inobaya MT, Olveda RM, Chau TN, Olveda DU, Ross AG, Prevention and control of schistosomiasis: a current perspective, *Res Rep Trop Med* **5**:65–75, 2014.
17. Spear DC, Hubbard A, Liang S, Seto E, Disease transmission models for public health decision making: toward an approach for designing intervention strategies for Schistosomiasis japonica, *Environ Health Perspect* **110**(9):907–915, 2002.
18. Wu J, Dhingra R, Gambhir M, Remais JV, Sensitivity analysis of infectious disease models: methods, advances and their application, *J R Soc Interface* **10**(86):20121018, 2013.
19. Xiang J, Chen H, Ishikawa H, A mathematical model for the transmission of Schistosoma japonicum in consideration of seasonal water level fluctuations of Poyang Lake in Jiangxi, China, *Parasitol Int* **62**(2):118–126, 2013.
20. Hussein ANA, Hassan IM, Khalifa R, Development and hatching mechanism of Fasciola eggs, light and scanning electron microscopic studies, *Saudi J Biol Sci* **17**(3):247–251, 2010.
21. McManus DP, Loukas A, Current status of vaccines for schistosomiasis, *Clin Microbiol Rev* **21**(1):225–242, 2008.
22. World Health Organization, Preventive Chemotherapy and Transmission Control, Department of Control of Neglected Tropical Diseases, 2010, Available at http://www.who.int/neglected_diseases/preventive_chemotherapy/databank/CP_Ghana.pdf (accessed August 2017).
23. World Health Organization, Schistosomiasis: population requiring preventive chemotherapy and number of people treated in 2015, Weekly Epidemiological Record, 2015, Available at http://www.who.int/wer/2015/wer9005.pdf (accessed June 2016).
24. MacDonald G, The dynamics of helminth infections, with special reference to schistosomes, *Trans R Soc Trop Med Hyg* **59**:489–506, 1965.
25. Hairston NG, An analysis of age-prevalence data by catalytic models. A contribution to the study of bilharziasis, *Bull World Health Organ* **33**:163–175, 1965.

26. Fine PEM, Lehman JS, Mathematical models of schistosomiasis: report of a workshop, *Am J Trop Med Hyg* **26**:500–504, 1977.
27. Nåsell I, Mathematical Models of Schistosomiasis, in El Tom MEA (ed.), *Developing Mathematics in Third World Countries*, North-Holland Publishing Company, Amsterdam, pp. 111–126, 1979.
28. Barbour AD, Schistosomiasis, in Anderson RM (ed.), *Population Dynamics of Infectious Diseases*, Chapman and Hall, London, pp. 180–208, 1982.
29. Bailey NTJ, The case for mathematical modelling of schistosomiasis, *Parasitol Today* **2**:158–163, 1986.
30. Castillo-Chavez C, Feng Z, Xu D, A schistosomiasis model with mating structure and time delay, *Math Biosci* **211**(2):333–341, 2008.
31. Diaby M, Iggidr A, Mamadou S, Abdou S, Global analysis of a schistosomiasis infection model with biological control, *Appl Math Comput* **246**:731–742, 2014.
32. Chiyaka ET, Magombedze G, Mutimbu L, Modelling within host parasite dynamics of schistosomiasis, *Comput Math Methods Med* **11**(5):255–280, 2010.
33. Garira W, Mathebula D, Netshikweta R, A mathematical modelling framework for linked within-host and between-host dynamics for infections with free-living pathogens in the environment, *Math Biosci* **256**:58–78, 2014.
34. Feng Z, Eppert A, Milner FA, Minchella DJ, Estimation of parameters governing the transmission dynamics of schistosomes, *Appl Math Lett* **17**(10):1105–1112, 2004.
35. Riley S, Carabin H, Marshall C, Olveda R, Willingham AL, McGarvey ST, Estimating and modeling the dynamics of the intensity of infection with Schistosoma japonicum in villagers of Leyte, Philippines. Part II: intensity specific transmission of S. japonicum. The schistosomiasis transmission and ecology project, *Am J Trop Med Hyg* **72**(6):754–761, 2005.
36. Mangal TD, Paterson S, Fenton A, Predicting the impact of long-term temperature changes on the epidemiology and control of schistosomiasis: a mechanistic model, *PLoS One* **3**(1):e1438, 2008.
37. Ghana population 2017, CountryMeters, Available at http://countrymeters.info/en/Ghana (accessed May 2017).
38. Chiyaka E, Garira W, Mathematical analysis of the transmission dynamics of schistosomiasis in the human-snail hosts, *J Biol Syst* **17**:397–423, 2009.
39. Ngarakana-Gwasira ET, Bhunu CP, Masocha M, Mashonjowa E, Transmission dynamics of schistosomiasis in Zimbabwe: a mathematical and GIS approach, *Commun Nonlinear Sci Numer Simul* **35**:137–147, 2016.
40. Ding C, Tao N, Sun Y, Zhu Y, The effect of time delays on transmission dynamics of schistosomiasis, *Chaos Solitons Fractals* **91**:360–371, 2016.
41. Pontryagin LS, Boltyanskii VG, Gamkrelidze RV, Mishchenko EF, *The Mathematical Theory of Optimal Processes*, Wiley, New York, 1962.
42. Zaman G, Yong HK, Jung IH, Stability analysis and optimal vaccination of an SIR epidemic model, *BioSystems* **93**:240–249, 2008.
43. Okosun KO, Ouifki R, Marcus N, Optimal control strategies and cost-effectiveness analysis of a malaria model, *BioSystems* **111**:83–101, 2013.
44. Zhang H, Georgescu P, Hassan AS, Mathematical insights and integrated strategies for the control of Aedes aegypti mosquito, *Appl Math Comput* **273**:1059–1089, 2016.
45. Liberatos JD, Schistosoma mansoni: male-biased sex ratios in snails and mice, *Exp Parasitol* **64**:165–177, 1987.
46. Beltram S, Boissier J, Male-biased sex ratio: why and what consequences for the genus Schistosoma, *Trends Parasitol* **26**:63–69, 2009.
47. Henderson J, Luca R, *Boundary Value Problems for Systems of Differential, Difference and Fractional Equations*, Elsevier, Amsterdam, 2015.

48. Feng Z, Li CC, Milner FA, Schistosomiasis models with density dependence and age of infection in snail dynamics, *Math Biosci* **177**:271–86, 2002.
49. Diekmann O, Heesterbeek JAP, Metz JAJ, On the definition and the computation of the basic reproduction ratio R_0 in models for infectious diseases in heterogeneous populations, *J Math Biol* **28**(4):365–382, 1990.
50. van den Driessche P, Watmough J, Reproduction numbers and sub-threshold endemic equilibria for compartmental models of disease transmission, *Math Biosci* **180**(1–2):29–48, 2002.
51. Castillo-Chavez C, Song B, Dynamical models of tuberculosis and their applications, *Math Biosci Eng* **1**(2):361–404, 2004.
52. Chitnis N, Hyman JM, Cushing JM, Determining important parameters in the spread of malaria through the sensitivity analysis of a mathematical model, *Bull Math Biol* **70**:1272–1296, 2008.
53. Dimitriu G, Boiculese VL, Sensitivity Study for a SEIT Epidemic Model, in *Proceedings of the 2015 E-Health and Bioengineering Conference* (*EHB*), *Iaşi*, IEEE Publishing, pp. 1–4, 2015.
54. Webster JP, Gower CM, Norton AJ, Evolutionary concepts in predicting and evaluating the impact of mass chemoterapy schistosomiasis control programmes on parasites and their hosts, *Evol Appl* **1**:66–83, 2008.
55. Alonso D, Munoz J, Gascon J, Valls ME, Corachan M, Failure of standard treatment with praziquantel in two returned travelers with Schistosoma haematobium infection, *Am J Trop Med Hyg* **74**:342–344, 2006.
56. Webster JP, Gower CM, Blair L, Do hosts and parasite coevolve? Empirical support from the Schistosoma system, *Am Nat* **164**:S33–S51, 2004.
57. Der EM, Quayson SE, Mensah JE, Tettey Y, Tissue schistosomiasis in accra ghana: a retrospective histopathologic review at the korle-bu teaching hospital (2004–2011), *Pathol Discov* **3**:1, 2015.
58. Sokolow S, Rickards C, The History of Schistosomiasis in Ghana, Available at http://schisto.stanford.edu/pdf/Ghana.pdf (accessed May 2017).

Appendix A. The Proof of Theorem 3.2

Proof. We shall express all coordinates of E^*, together with λ_H^*, λ_v^*, in terms of I_H^*. From the equilibrium relations (3.3)–(3.5), it follows that

$$\lambda_H^* = \frac{\mu_H(\mu_H+\psi_H)(\mu_H+\delta_H+\kappa_H)I_H^*}{\Lambda_H\psi_H - [(\mu_H+\psi_H)(\mu_H+\delta_H+\kappa_H)-\kappa_H\psi_H]I_H^*}, \tag{A.1}$$

$$S_H^* = \frac{\Lambda_H\psi_H - [(\mu_H+\psi_H)(\mu_H+\delta_H+\kappa_H)-\kappa_H\psi_H]I_H^*}{\mu_H\psi_H}. \tag{A.2}$$

From the equilibrium relations (3.4), (3.5), (3.9)–(3.13), using the notation

$$P^* = \frac{(1-\tau)\omega\alpha_c}{\alpha_c+\mu_c}\cdot\frac{\alpha_I}{\alpha_I+\mu_I}\cdot\frac{N_m\alpha_m}{\alpha_m+\mu_m}\cdot\frac{N_e\alpha_e}{\alpha_e+\mu_e}\cdot\frac{1}{2},$$

one obtains that

$$M^* = P^*\cdot\frac{(\mu_H+\psi_H)(\mu_H+\delta_H+\kappa_H)}{\mu_p\psi_H}I_H^*. \tag{A.3}$$

From (3.15), one sees that

$$C^* = \frac{C_0}{\frac{\beta_H}{\lambda_H^*} - 1}.$$

Using the notation

$$T_H = \beta_H[(\mu_H + \psi_H)(\mu_H + \delta_H + \kappa_H) - \kappa_H\psi_H] + \mu_H(\mu_H + \psi_H)(\mu_H + \delta_H + \kappa_H),$$

we may use the explicit expression of λ_H^* in terms of I_H^* given by (A.1) to express C^* in terms of I_H^* as well, in the form

$$C^* = \frac{C_0\mu_H(\mu_H + \psi_H)(\mu_H + \delta_H + \kappa_H)I_H^*}{\beta_H\Lambda_H\psi_H - T_HI_H^*}. \tag{A.4}$$

From the equilibrium relations (3.8) and (3.14), it follows that

$$E_v^* = \frac{\mu_v + \delta_v}{\phi_v} \cdot \frac{\mu_s C^*}{N_s\gamma_s}. \tag{A.5}$$

Using the equilibrium relations (3.6), (3.7) together with (A.5), it is seen that

$$S_v^* = \frac{\Lambda_v\phi_vN_s\gamma_s - (\mu_v + \delta_v + \phi_v)(\mu_v + \delta_v)\mu_sC^*}{\mu_v\phi_vN_s\gamma_s}, \tag{A.6}$$

$$\lambda_v^* = \frac{(\mu_v + \delta_v + \phi_v)(\mu_v + \delta_v)\mu_s\mu_vC^*}{\Lambda_v\phi_vN_s\gamma_s - (\mu_v + \delta_v + \phi_v)(\mu_v + \delta_v)\mu_sC^*}. \tag{A.7}$$

From (A.7), it follows that

$$\lambda_v^* = \frac{\mu_v}{\frac{\Lambda_v\phi_vN_s\gamma_s}{(\mu_v+\delta_v+\phi_v)(\mu_v+\delta_v)\mu_sC^*} - 1},$$

which, combined with (3.16) leads to

$$\beta_vM^* \cdot \frac{\Lambda_v\phi_vN_s\gamma_s}{(\mu_v + \delta_v + \phi_v)(\mu_v + \delta_v)\mu_sC^*} - \beta_vM^* = (M_0 + M^*)\mu_v.$$

Substituting now the expressions of M^* and C^* given by (A.3) and (A.4), respectively, one obtains that

$$\begin{aligned}&\frac{R_0^2M_0\mu_v}{\beta_H\Lambda_H\psi_H}(\beta_H\Lambda_H\psi_H - T_HI_H^*)\\ &\quad = P^*\frac{(\mu_H + \psi_H)(\mu_H + \delta_H + \kappa_H)}{\mu_p\psi_H}(\beta_v + \mu_v)I_H^* + M_0\mu_v,\end{aligned} \tag{A.8}$$

which leads to

$$I_H^* = \frac{M_0\mu_v(R_0^2 - 1)}{P^*\frac{(\mu_H+\psi_H)(\mu_H+\delta_H+\kappa_H)}{\mu_p\psi_H}(\beta_v + \mu_v) + \frac{R_0^2M_0\mu_v}{\beta_H\Lambda_H\psi_H}T_H}.$$

It then follows that I_H^* is positive (and unique) if and only if $R_0 > 1$. Let us now suppose that $R_0 > 1$. From (3.5), it also follows that E_H^* is positive. From (A.8),

one sees that

$$\beta_H \Lambda_H \psi_H > T_H I_H^*,$$

which implies that

$$\Lambda_H \psi_H > [(\mu_H + \psi_H)(\mu_H + \delta_H + \kappa_H) - \kappa_H \psi_H] I_H^*.$$

From (A.1) and (A.2), it also follows that S_H^* and λ_H^* are positive. From (3.9)–(3.13), one obtains that C_H^*, W_I^*, W_m^*, e_H^*, E_L^*, E_W^*, M^* are positive. Now, from (3.16), it also follows that λ_v^* is positive, and using (3.6)–(3.8), it is seen that S_v^*, E_v^*, I_v^* are positive, which finishes the proof. □

Appendix B. Proof of Theorem 3.3

Proof. The Jacobian matrix $J(E^0)$ of (3.17) computed at β^* has a right eigenvector associated with the eigenvalue 0, given by $w = (w_1, w_2, w_3, w_4, w_5, \ldots, w_{12})^T$, in which

$$\begin{aligned}
w_1 &= \frac{\beta^* \Lambda_H}{\mu_H C_0 \mu_H} - \frac{\kappa_H \beta^* \Lambda_H \psi_H}{\mu_H(\mu_H + \delta_H + \kappa_H) C_0 \mu_H (\mu_H + \psi_H)},\\
w_2 &= \frac{\beta^* \Lambda_H}{C_0 \mu_H (\mu_H + \psi_H)}\\
w_3 &= \frac{\beta^* \Lambda_H \psi_H}{(\mu_H + \delta_H + \kappa_H) C_0 \mu_H (\mu_H + \psi_H)},\\
w_4 &= -\frac{(\mu_v + \delta_v + \phi_v)(\mu_v + \delta_v)\mu_s}{\mu_v N_s \gamma_s \phi_v},\\
w_5 &= \frac{(\mu_v + \delta_v)\mu_s}{N_s \gamma_s \phi_v},\\
w_6 &= \frac{\mu_s}{N_s \gamma_s},\\
w_7 &= \frac{(1-\tau)\omega \beta^* \Lambda_H}{C_0 \mu_H (\alpha_c + \mu_c)},\\
w_8 &= \frac{(1-\tau)\omega \beta^* \Lambda_H \alpha_c}{C_0 \mu_H (\alpha_I + \mu_I)(\alpha_c + \mu_c)},\\
w_9 &= \frac{(1-\tau)\omega \beta^* \Lambda_H \alpha_I \alpha_c}{2 C_0 \mu_H (\alpha_I + \mu_I)(\alpha_m + \mu_m)(\alpha_c + \mu_c)},\\
w_{10} &= \frac{(1-\tau)\omega \beta^* \Lambda_H N_m \alpha_m \alpha_c \alpha_I}{2 C_0 \mu_H (\alpha_I + \mu_I)(\alpha_m + \mu_m)(\alpha_c + \mu_c)(\alpha_e + \mu_e)},\\
w_{11} &= \frac{(1-\tau)\omega \beta^* \Lambda_H N_m \alpha_m \alpha_c \alpha_I N_e \alpha_e}{2 C_0 \mu_H (\alpha_I + \mu_I)(\alpha_m + \mu_m)(\alpha_c + \mu_c)(\alpha_e + \mu_e)\mu_p},\\
w_{12} &= 1.
\end{aligned}$$

The left eigenvector associated with the eigenvalue 0 is $v = (v_1, v_2, v_3, \ldots, v_{12})$, where

$$
\begin{aligned}
v_1 &= v_2 = v_3 = v_4 = 0,\\
v_5 &= \frac{\phi_v N_s \gamma_s}{(\mu_v + \delta_v + \phi_v)(\mu_v + \delta_v)},\\
v_6 &= \frac{N_s \gamma_s}{(\mu_v + \delta_v)},\\
v_7 &= \frac{\alpha_c \alpha_I N_m \alpha_m N_e \alpha_e \beta^* g \Lambda_v \phi_v N_s \gamma_s}{(\alpha_c + \mu_c)(\alpha_I + \mu_I)(\alpha_m + \mu_m)(\alpha_e + \mu_e)\mu_p M_0 \mu_v (\mu_v + \delta_v + \phi_v)(\mu_v + \delta_v)},\\
v_8 &= \frac{\alpha_I N_m \alpha_m N_e \alpha_e \beta^* g \Lambda_v \phi_v N_s \gamma_s}{(\alpha_I + \mu_I)(\alpha_m + \mu_m)(\alpha_e + \mu_e)\mu_p M_0 \mu_v (\mu_v + \delta_v + \phi_v)(\mu_v + \delta_v)},\\
v_9 &= \frac{N_m \alpha_m N_e \alpha_e \beta^* g \Lambda_v \phi_v N_s \gamma_s}{(\alpha_m + \mu_m)(\alpha_e + \mu_e)\mu_p M_0 \mu_v (\mu_v + \delta_v + \phi_v)(\mu_v + \delta_v)},\\
v_{10} &= \frac{N_e \alpha_e \beta^* g \Lambda_v \phi_v N_s \gamma_s}{(\alpha_e + \mu_e)\mu_p M_0 \mu_v (\mu_v + \delta_v + \phi_v)(\mu_v + \delta_v)},\\
v_{11} &= \frac{\beta^* g \Lambda_v \phi_v N_s \gamma_s}{\mu_p M_0 \mu_v (\mu_v + \delta_v + \phi_v)(\mu_v + \delta_v)},\\
v_{12} &= 1.
\end{aligned}
$$

The associated second order partial derivatives at the disease-free equilibrium for the system (3.17) are given by

$$
a = \sum_{k,i,j=1}^{12} v_k w_i w_j \frac{\partial^2 h_k}{\partial x_i \partial x_j}(E^0, \beta^*),
$$

$$
b = \sum_{k,i=1}^{12} v_k w_i \frac{\partial^2 h_k}{\partial x_i \partial \beta_H}(E^0, \beta^*).
$$

Since $v_k = 0$ for $k = 1, 2, 3, 4$, we consider v_k for $k = 5, 6, 7, 8, 9, 10, 11, 12$. From system (3.19), the following functions will be used to compute a and b:

$$
h_5 = \frac{g\beta^* x_{11} x_4}{M_0 + x_{11}} - (\mu_v + \delta_v + \phi_v) x_5, \tag{B.1}
$$

$$
h_7 = \frac{(1-\tau)\omega\beta^* x_{12} x_1}{C_0 + x_{12}} - (\alpha_c + \mu_c) x_7. \tag{B.2}
$$

Hence,

$$
\begin{aligned}
\frac{\partial^2 h_5}{\partial x_4 \partial x_{11}} &= \frac{g\beta^*}{M_0},\\
\frac{\partial^2 h_7}{\partial x_1 \partial x_{12}} &= \frac{(1-\tau)\omega\beta^*}{C_0},
\end{aligned}
$$

$$\frac{\partial^2 h_5}{\partial x_{11}^2} = -\frac{2g\beta^*\Lambda_v}{M_0^2\mu_v},$$
$$\frac{\partial^2 h_7}{\partial x_{12}^2} = -\frac{2(1-\tau)\omega\beta^*\Lambda_H}{C_0^2\mu_H}.$$

Therefore,

$$a = -\frac{M_0\mu_p\mu_v}{\Lambda_v}(M_0\mu_v\mu_s\mu_p R_{0H} + 2R_0^2)$$
$$- 2R_0^2\left(\frac{\kappa_H\psi_H\beta^*\Lambda_H(1-\tau)\omega\beta^*}{C_0^2\mu_H^2(\mu_H+\psi_H)(\mu_H+\delta_H+\kappa_H)} - \frac{R_{0H}\mu_s}{\mu_H C_0}\right) < 0.$$

Similarly, from Eqs. (B.1) and (B.2), we have

$$\frac{\partial^2 h_5}{\partial x_{11}\partial\beta_H} = \frac{g\Lambda_v}{M_0\mu_v},$$
$$\frac{\partial^2 h_7}{\partial x_{12}\partial\beta_H} = \frac{(1-\tau)\omega\Lambda_H}{C_0\mu_H}.$$

Therefore,

$$b = R_0^2\left(\frac{\mu_p\mu_s}{\beta^*} + \frac{(1-\tau)\omega\Lambda_H}{C_0\mu_H}\right) > 0.$$

Hence, $a < 0$ and $b > 0$. Applying Theorem 4.1 (iv) in Ref. 51, we then obtain that the endemic equilibrium E^* is locally asymptotically stable for $R_0 > 1$, but close to 1. □

Appendix C. Certain Sensitivity Indices of R_0

(i) The sensitivity index of R_0 with respect to μ_v

$$\Upsilon_{\mu_v}^{R_0} = \frac{\mu_v}{R_0}\cdot\frac{\partial R_0}{\partial\mu_v} = -2;$$

(ii) The sensitivity index of R_0 with respect to β_v

$$\Upsilon_{\beta_v}^{R_0} = \frac{N_s\gamma_s\Lambda_v\beta_v(\mu_v+\delta_v+\phi_v)\mu_v M_0\mu_p}{\mu_v M_0\mu_p(\mu_v+\delta_v+\phi_v)N_s\gamma_s\Lambda_v\beta_v}.$$

(iii) The sensitivity index of R_0 with respect to μ_c

$$\Upsilon_{\mu_c}^{R_0} = -\frac{\mu_c}{\alpha_c+\mu_c}.$$

(iv) The sensitivity index of R_0 with respect to α_w

$$\Upsilon_{\alpha_w}^{R_0} = \frac{\mu_w}{\alpha_w+\mu_w}.$$